Donecopride, a Swiss army knife with potential interest against Alzheimer's disease

Christophe Rochais, Cédric Lecoutey, Katia Hamidouche, Patrizia Giannoni, Florence Gaven, Eleazere Cem, Serge Mignani, Kévin Baranger, Thomas Freret, Joël Bockaert, et al.

Donecopride, a Swiss army knife with potential interest against Alzheimer's disease

Running title: **Donecopride, a Swiss army knife against AD**

Christophe Rochais[a,b], Cédric Lecoutey[a,b], Katia Hamidouche[a,c], Patrizia Giannoni[d,1], Florence Gaven[d,2], Eleazere Cem[d], Serge Mignani[a,b], Kevin Baranger[e], Thomas Freret[a,c], Joël Bockaert[d], Santiago Rivera[e], Michel Boulouard[a,c], Patrick Dallemagne[a,b,3], Sylvie Claeysen[d,3]

[a]Normandie Univ, F-14032 Caen, France; [b]UNICAEN, CERMN (Centre d'Etudes et de Recherche sur le Médicament de Normandie), F-14032 Caen, France; [c]UNICAEN, INSERM U1075 COMETE F-14032 Caen, France; [d]IGF, Univ Montpellier, CNRS, INSERM, F-34094, Montpellier, France; [e]Aix-Marseille Univ, CNRS, INP, Inst Neurophysiopathol,F-13344, Marseille, France

[1]Present address: Equipe Chrome, EA7352, Université de Nîmes, F-30000 Nîmes, France.
[2]Present address: CRBM, CNRS UMR5237, F-34293 Montpellier cedex 5, France.
[3]P.D. and S. C. contributed equally to this work.

Corresponding authors:
Patrick Dallemagne
CERMN – EA4258
Boulevard Becquerel, 14032 Caen, France
+33 231 566 813
Email: patrick.dallemagne@unicaen.fr

Sylvie Claeysen
IGF – CNRS UMR5203 – INSERM U1191 – Univ. Montpellier
141 rue de la Cardonille, 34094 Montpellier cedex 5, France
+33 434 359 215
Email: sylvie.claeysen@igf.cnrs.fr

Author contributions: C.R., T.F., M.B., P.D., and S.C. designed research; C.L., K.H., P.G., F.G., E.C., and K.B. performed research; C.R., T.F., J.B., S.M., S.R., M.B., P.D., and S.C. analyzed data; and C.R., S.C., and P.D. wrote the paper.

The authors declare no conflict of interest.

Abstract

Background and Purpose

We recently identified donecopride as a pleiotropic compound able to inhibit acetylcholinesterase and to activate serotonin subtype 4 receptor. The purpose of the present article is to establish its potential therapeutic interest against Alzheimer's disease (AD).

Experimental approach

The present work used both *in cellulo* and *in vivo* models of AD.

Key Results

In the present study, we show that, in vivo under chronic administration, donecopride displays potent anti-amnesic properties in two different animal models of Alzheimer's disease (AD) (transgenic 5XFAD mice and mice exposed to soluble amyloid-β peptides). Donecopride preserved learning capacities, including working and long-term spatial memories, which were evaluated with various behavioral tests (novel object recognition, Y-maze, Morris water maze). These behavioral observations found molecular correlation with the interactions of donecopride related to the two main types of molecular damage in AD. Indeed, a decrease in amyloid aggregation was observed in the brain of the treated transgenic mice, as well as a reduction in tau hyperphosphorylation in rat primary cultures of hippocampal neurons. At the cellular level, donecopride exerted neuroprotective effects toward neurons and the neurite network, as well as neurotrophic benefits, expressed as the formation of new synapses.

Conclusions & Implications

Pleiotropic donecopride acts like a Swiss army knife, displaying sustainable symptomatic therapeutic effects and potential disease-modifying roles against AD. Clinical trials with this promising drug candidate will soon be undertaken to confirm its therapeutic potential in humans.

Keywords: Alzheimer; donecopride; MTDL; pleiotropic

Introduction

For 20 years, no new drug has been marketed against Alzheimer's disease (AD). Those that are available, mainly the acetylcholinesterase (AChE) inhibitors (AChEIs), display only symptomatic and transient therapeutic benefits because their mechanism of action is to target an enzyme condemned to disappear as neurodegeneration progresses (Melnikova, 2007; Rosini *et al.*, 2014; Citron, 2010). None of the countless novel target/drug combinations evaluated in clinical trials to date have successfully produced an efficient disease-modifying effect. Among the possible explanations for these failures, most difficulties lie in i) the selection of patients in a clinical state that allows them to benefit from the potential treatment; ii) the development of relevant animal models of AD, and iii) the multifactorial origin of the disease, which warrants a multitarget approach (reviewed in Cavalli *et al.*, 2008; Schmitt *et al.*, 2004). The latter consideration has now been taken into account, as most current clinical trials against AD combine donepezil – the most widely used AChEI on the market – with the novel drug being tested (Frolich et al, 2019).

Our consortium pursues such a multitarget approach by using multitarget-directed ligands (MTDLs), which are specifically designed to reach several targets and to consequently display synergistic effects without the risk inherent in drug associations and drug-drug interactions. We recently chose to target both the serotonergic subtype 4 receptor (5-HT_4R) in order to exert a potential neuroprotective effect and AChE (Lecoutey *et al.*, 2014; Rochais *et al.*, 2015), whose inhibition remains relevant when associated with a protective effect of the targeted enzyme (Wang and Zhang 2019).

On the one hand, activation of 5-HT_4R allows both the release of acetylcholine (Kilbinger and Wolf, 1992) and the activation of an α-secretase. The latter promotes non-amyloidogenic cleavage of the amyloid precursor protein (APP) to generate the neurotrophic soluble APPα (sAPPα) protein in a manner that is detrimental for the formation of the neurotoxic amyloid-β (Aβ) peptide (Maillet *et al.*, 2003; Cho and Hu, 2007). On the other hand, inhibiting the catalytic active site of AChE preserves neurotransmitter release (Musial *et al*, 2007). If this effect occurs through interaction with the peripheral anionic site of AChE, the enzyme is not able to form aggregates with soluble Aβ peptides, decreasing the neurotoxic feature displayed by amyloids (Inestrosa *et al*, 1996).

Our group recently succeeded in combining these activities into a sole pleiotropic compound named donecopride, which is potentially able to display both symptomatic and

disease-modifying therapeutic effects in the treatment of AD (Lecoutey *et al.*, 2014; Rochais *et al.*, 2015).

Donecopride is a selective, partial (48.3%), nanomolar (Ki = 8.5 nM) (*h*)5-HT_4R agonist, which promotes the release of soluble APPα in vitro and in vivo (Lecoutey *et al.*, 2014; Rochais *et al.*, 2015). It also behaves as a mixed-type competitive (*h*)AChEI (IC_{50} = 16 nM) that is selective toward butyrylcholinesterase and that partially displaces propidium iodide from the peripheral anionic site, accounting for a potential inhibitory effect against AChE-induced Aβ aggregation. Further, in NMRI mice in vivo, with an i.p. dose of 0.3 mg/kg, donecopride displayed procognitive effects, as established in the novel object recognition (NOR) test, and antiamnesic effects by the reversion of scopolamine-induced memory impairments, as shown in the spontaneous alternation test (Lecoutey *et al.*, 2014).

This pharmacological profile led us to test the therapeutic potential of donecopride against AD by using two complementary animal models: i) the 5XFAD transgenic mouse model and ii) a mouse model of AβO intracerebroventricular (i.c.v.) injections. In 5XFAD mice, the more intense amyloid-producing mouse model, we assayed the potential of donecopride to prevent amyloid production and associated cognitive impairment. The AβO-injected mice were used to demonstrate the ability of donecopride to challenge amyloid acute toxicity and to be effective when administered p.o. Finally, we attempted to correlate the observed in vivo activities of donecopride with a potential neuroprotective effect measured in cellulo on rat hippocampal neurons exposed to AβO. We herein report the results of this study.

Materials and Methods

Details describing the 5XFAD experiments (quantification of Aβ, NOR test, quantification of senile plaques, quantification of GFAP), experiments using soluble Aβ peptides (Y-maze test, MWM test, NOR test), and rat hippocampal neuron culture experiments can be found in *SI Text*.

Data and statistical analysis

The data and statistical analysis comply with the recommendations of the British Journal of Pharmacology on experimental design and analysis in pharmacology (Curtis *et al.*, 2018). Studies were designed to generate groups of equal size and mice were randomly assigned in the experimental groups. Group size may vary according to power analysis and expertise of the authors regarding the behavioral tests used: NOR test, Y-maze test and MWM test (Leger *et al.* 2013; Freret *et al.* 2012; Freret *et al.* 2017). Mice were submitted to behavioral experiments in a randomized sequential order. Behavioral recordings and immunofluorescence images were

blindly analyzed. Culture data were automatically acquired. Statistical analysis was undertaken only for studies where each group size was at least n = 5. Group size is the number of independent values and statistical analysis was done using these independent values. All values are expressed as the mean ± SEM. Statistical analyses were performed using GraphPad Prism 8.01 (GraphPad Software, La Jolla, CA, USA, RRID:SCR_002798). Statistical tests used are indicated in the legends of the figures. In each dataset, Gaussian distribution was verified (Shapiro–Wilk normality test) and the homogeneity of sample variance was tested using both Brown–Forsythe's and Bartlett's tests. As long as no variance among groups was detected, ANOVA was performed. Grouped analysis were performed using two-way ANOVA, followed by a Bonferroni's test for multiple comparisons. Paired group comparisons were processed by One-way ANOVA (post-hoc correction) or Student's t-test. Only probability values $p < 0.05$ were considered statistically significant. For GFAP studies and following the recommendations of the BJP guidelines (Curtis *et al.*, 2019), the GFAP data were log-transformed to obtain Gaussian distribution and keep the group with a n of equal size (n = 7). In as much as possible, untransformed data are presented. In the case of necessary normalisation, the Y-axis labelling and the legend explicit the transformation of the data. No outliers were removed in the present study. The immunofluorescence procedures used in this study comply with BJP Guidelines (Alexander *et al.*, 2018).

Nomenclature of Targets and Ligands

Key protein targets and ligands in this article are hyperlinked to corresponding entries in http://www.guidetopharmacology.org, the common portal for data from the IUPHAR/BPS Guide to PHARMACOLOGY (Harding *et al.*, 2018), and are permanently archived in the Concise Guide to PHARMACOLOGY 2017/18 (Alexander *et al.*, 2017).

Results

Chronic Administration of Donecopride Decreases the Amyloid Load in Soluble and Insoluble Fractions of 5XFAD Mouse Brains. 5XFAD transgenic mice overexpress mutant human APP(695) with the Swedish (K670N, M671L), Florida (I716V), and London (V717I) familial Alzheimer's disease (FAD) mutations, along with human PS1 harboring two FAD mutations, M146L and L286V (Oakley *et al.*, 2006). 5XFAD mice recapitulate major features of AD amyloid pathology, including amyloid-induced neurodegeneration, inflammation, and synaptic and behavioral dysfunction (Crouzin *et al.*, 2013; Girard *et al.*, 2014; Giannoni *et al.*

2013, 2016). In a first experiment conducted under the original B6/SJL genetic background (Oakley *et al*., 2006,; Giannoni *et al.,* 2016), female mice received vehicle or donecopride (1 mg/kg) by i.p. administration twice a week for 3 mo from 10 to 22 wk of age. The treatment started when amyloid plaques began to appear in mouse brains (Crouzin et al.; 2013). $A\beta_{40}$ and $A\beta_{42}$ were quantified from brain extracts in soluble and insoluble fractions (Fig. 1). In both fractions, donecopride was able to significantly reduce $A\beta_{42}$ levels without any change in $A\beta_{40}$ levels.

Chronic Administration of Donecopride Prevents Memory Impairments and Decreases Amyloid Plaques and Astrogliosis in some brain regions in 5XFAD Mice. In a second set of experiments conducted on mice with the C57BL/6J genetic background (more appropriate for behavioral studies), female 5XFAD mice received vehicle or donecopride (1 mg/kg) by i.p. administration twice a week for 3 mo from 11 to 22 wk of age. The treatment started when amyloid deposits began to form in mouse brains (Oakley *et al*., 2006,; Giannoni *et al.,* 2016). At the end of treatment, mice were evaluated with the NOR test for long-term memory performance. This test assesses recognition memory for objects, its human equivalent being the visual paired-comparison task (Wallace *et al.*, 2015). The recognition of objects is mediated by the perirhinal cortex in rodents (Brown *et al.*, 2012; Albasser *et al.,* 2009; 21-23; Norman et Eacott; 2005), primates (Zeamer *et al.*; 2015), and humans (Watson and Lee, 2013). AD pathology develops in the perirhinal and entorhinal cortex before it appears in the hippocampus (deToledo-Morrell *et al.*, 2004; Stoub *et al.*, 2005; Taylor *et al.*, 2008). The visual paired-comparison task detects memory deficits in patients with mild cognitive impairment (Lagun *et al.*, 2011) and predicts conversion from this condition to AD (Zola *et al.*, 2013).

Habituation sessions were started 3 d after the end of treatment to avoid interference with acute effects. The interval between the training session and the test was 24 h. During training sessions (Fig.2A), two-way repeated-measures ANOVA demonstrated that the animals presented neither preference for the objects ($F_{(1,12)} = 1.90$; NS) nor difference due to the treatment ($F_{(1,12)} = 1.22$; NS). However, during test sessions (Fig. 2B), a significant group difference appeared between 5XFAD-vehicle and 5XFAD-donecopride treated groups regarding object discrimination ($F_{(1,12)} = 10.77$; $p < 0.05$) with no treatment-group difference ($F_{(1,12)} = 1.27$; NS) and no interaction between treatment group and object ($F_{(1,12)} = 1.51$; NS). Vehicle-treated mice presented impaired memory performance and were not able to discriminate novel objects from familiar objects, as shown by similar exploration times for both

objects (Fig. 2B) and by the nonsignificant discrimination index (Fig. 2C). Donecopride prevented cognitive impairment, as indicated by the higher time devoted to exploration of the novel object in mice treated with donecopride in comparison with mice treated with vehicle (Fig. 2B). The discrimination index of the compound-treated group was different from 0 (chance level) (Fig. 2C). The total exploration time during the training session did not differ significantly between the two groups (Fig. 2D), indicating that improvement of recognition memory in 5XFAD mice treated with donecopride was not secondary to an increase in exploratory activity.

The frontal cortex, hippocampus, and entorhinal cortex were analyzed as representative areas of 5XFAD mouse brains (frontal, median, and caudal sections) and of human brain regions that are affected by AD early and are highly enriched in amyloid deposits. Donecopride treatment significantly decreased the number of amyloid plaques compared with vehicle in the frontal cortex (reduction of 16 ± 3%) (Fig. 3A) and the entorhinal cortex (reduction of 24 ± 4%) (Fig. 3C). The number of amyloid plaques in the hippocampus of 5XFAD mice treated with donecopride was not significantly different than that in controls (Fig. 3B).

Immunohistochemical assessment of the astroglial cell population [glial fibrillary acidic protein (GFAP) staining] showed that chronic donecopride treatment significantly reduced astrogliosis in entorhinal brain slices of treated animals in comparison to controls (Fig. 3G, H). Despite a tendency to reduce astrogliosis in the hippocampus and the frontal cortex, however, donecopride treatment did not reach statistical significance in these brain areas (Fig. 3E, F).

Collectively, the data obtained in 5XFAD mice demonstrated that donecopride is able to prevent long-term deficits in recognition memory. This effect was associated with a decrease in amyloid pathology and in astrogliosis in some brain regions.

Subchronic Administration of Donecopride Prevents Memory Impairments in Soluble Aβ Peptides-Injected C57BL/6 Mice. Donecopride was then investigated in a preclinical AD model with wild-type C57BL/6J mice (3 mo of age) challenged at day 0 with an i.c.v. injection of soluble $A\beta_{1-42}$ peptides to induce neuronal death in vitro and cognitive decline in vivo (Pillot *et al.*, 1999; Kriem *et al.*, 2005; Malaplate-Armand *et al.*, 2006; Youssef *et al.*, 2008; Garcia *et al.*, 2010; Desbene *et al.*, 2012). The neurotoxicity and associated cognitive deficits induced by soluble Aβ peptides involve the activation of neuroinflammatory processes, including activation of glial cells and production of pro-inflammatory cytokines, such as interleukin-1β

and tumor necrosis factor α. Donecopride and donepezil (used as a control) were administered p.o. (through oral gavage) once a day from day -1 to day +17 at three different doses. At day +4 (i.e. 4 d after disease induction), spatial working memory was assessed with the Y-maze test. From day +3 to day +14, learning capacities and long-term memory were investigated with the Morris water maze (MWM) assay. At days +15/+16, recognition memory was investigated with the NOR test (see Fig. S1 for time schedule of the experiments).

Spatial working memory (Y-maze test). The Y-maze test assesses spatial working memory, which is mainly mediated by the prefrontal cortex (working memory) and the hippocampus (spatial component) (Yoon *et al.*, 2008; Spellman *et al.*, 2015) and is decreased in AD (Benjamin *et al.*, 2015; Bianchini *et al.*, 2014; Schroeter *et al.*, 2012). The measurement of spontaneous alternation behavior has been widely used by behavioral pharmacologists to assess spatial working memory, a component of short-term memory (Sarter *et al.*, 1988). In its simplest form, spontaneous alternation behavior is the tendency of mice to alternate their conventional non-reinforced choice of maze arms on successive opportunities. The i.c.v. infusion of soluble Aβ peptides induces cognitive deficits in this test (Youssef *et al.*, 2008; Garcia *et al.*, 2010; Desbene *et al.*, 2012; Bouter *et al.*, 2013).

In the Y-maze test, one-way ANOVA revealed a treatment effect ($F_{(6, 76)} = 2.668$; $p < 0.05$) regarding alternation behavior. At a dose of 3 mg/kg/d, donecopride rescued soluble Aβ peptides-induced impairment of spatial working memory, since treated mice exhibited alternation behavior that was similar to that shown by vehicle mice but different from that of soluble Aβ peptides-injected mice (pairwise comparison followed by Bonferroni's test, $p < 0.05$) (Fig. 4A). At 1 and 9 mg/kg/d and in the presence of soluble Aβ peptides, donecopride-treated mice exhibited an intermediate phenotype with an alternation behavior that was similar to that of both vehicle mice and soluble Aβ peptides-injected mice. In this experiment, donepezil also resulted in intermediate activity at a dose of 1 mg/kg/d and was not able to fully rescue the soluble Aβ peptides-induced impairment. The mice treated with donecopride alone at the dose of 9 mg/kg presented an alternation behavior, that was not significantly different from the vehicle-treated mice. In all groups, the number of arm entries was similar (ANOVA; $F_{(6, 76)} = 0.9176$; NS; Fig. 4B).

Learning capacities and long-term memory (MWM test). Spatial reference memory is a process that allows one to remember the spatial pathway to a specific location. It is mediated by the integrity of the hippocampus network in rodents (Broadbent *et al.*, 2006; Martin *et al.*,

2005; Mumby *et al.*; 1999) and in humans (Goodrich-Hunsaker *et al.*, 2010; Bartsch *et al.*, 2010), as shown on a virtual MWM task. Injection of soluble Aβ peptides i.c.v. in mice induces a deficit in spatial reference memory in the MWM (Youssef *et al.*, 2008; Garcia *et al.*, 2010; Desbene *et al.*, 2012; Bouter *et al.*, 2013).

The learning capacities of mice were monitored for 5 consecutive days-as indicated in Fig. S1. Regarding escape latency (Fig. 5A), two-way repeated-measures ANOVA revealed a time effect ($F_{(4, 308)} = 6.981$; $p < 0.05$) and a good matching of the measures ($F_{(77, 308)} = 1.999$; $p < 0.05$) but not treatment effect ($F_{(6, 77)} = 0.8076$; NS) and no treatment x time interaction ($F_{(24, 308)} = 0.7561$; NS). Administration of donecopride at a dose of 3 mg/kg/d resulted in improvement in learning capacities of these mice (escape latency difference at day 5 compared with day 1, Student's *t* test; $p < 0.05$) compared with those of soluble Aβ peptides-injected mice (difference from day 1, Student's *t* test; NS); donepezil appeared to be inactive at a dose of 1 mg/kg/d (difference from day 1, Student's *t* test; NS) (Fig. 5A). In absence of soluble Aβ peptides, donecopride at a dose of 9 mg/kg/d did not seem to alter the global learning performance of the mice (escape latency difference at day 5 compared with day 1, Student's *t* test; $p < 0.05$). The absence of effect of donecopride at a dose of 9 mg/kg/d to counteract Aβ-induced learning deficits (difference from day 1, Student's *t* test: NS) could be explained as the desensitization of 5-HT_4R, which is extremely rapid in neurons when the receptor is challenged with high doses of agonists (Ansanay *et al.*, 1992). We have previously demonstrated that this effect is mediated first by a G protein-coupled receptor kinase 2-dependent uncoupling of the receptor, followed by its β-arrestin-dependent endocytosis (Barthet *et al.*, 2005). Moreover, because the 5-HT_4R is not recycled, new biosynthesis of the receptor is necessary for its return to the plasma membrane, and repetitive high administration of an agonist could lead to a decrease or even a loss of response (Barthet *et al.*, 2005). We previously reported such a bell-shaped curve while investigating the effects of donecopride on scopolamine-induced impairment during the spontaneous alternation test (Rochais *et al.*, 2015).

Regarding the average swimming speed (Fig. 5B), two-way ANOVA with repeated measures revealed a time effect ($F_{(4, 308)} = 17.88$; $p < 0.05$) and a good matching of the measures ($F_{(77, 308)} = 3.524$; $p < 0.05$), but neither treatment effect ($F_{(6, 77)} = 1.584$; NS) nor treatment x time interaction ($F_{(24, 308)} = 0.7312$; NS), demonstrating thus no biased locomotor effect whatever the group considered.

Regarding the average traveled distance (Fig. 5C), two-way ANOVA with repeated-measures revealed a time effect ($F_{(4, 308)} = 7.798$; $p < 0.05$) and a good matching of the measures ($F_{(77, 308)} = 5.432$; $p < 0.05$), but neither treatment effect ($F_{(6, 77)} = 0.2091$; NS) nor treatment x

time interaction ($F_{(24, 308)} = 0.5272$; NS). Nevertheless, multiple comparisons demonstrated that the vehicle treated group was the only one to present a significant decrease in traveled distance (Bonferroni's test; $p < 0.05$).

Long-term memory performance was determined 2 d after the last training session and 14 d after i.c.v. injection of vehicle or soluble Aβ peptides. During the probe trial, the time at first cross (i.e., latency to target, Fig. 5D), the number of crossings over the former platform location (Fig. 5E) and the time in target quadrant (Fig. 5F) were determined. One-way ANOVA revealed a group effect in the latency to target ($F_{(6, 72)} = 3.040$; $p < 0.05$) and a significant effect of donecopride at 1 mg/kg/d (Bonferroni's post-test; $p < 0.05$). In the number of crossing, one-way ANOVA revealed also a group effect ($F_{(6, 73)} = 4.255$; $p < 0.05$) and donecopride (at all doses) inhibited soluble Aβ peptides-induced impairment of long-term memory (Bonferroni's post-test; $p < 0.05$). In that paradigm, donepezil at 1 mg/kg/d demonstrated no significant effect to prevent memory impairment, neither on latency to former platform location nor on number of crossings (Bonferroni's post-test; $p < 0.05$). The time spent in target quadrant was not significantly different between groups (one-way ANOVA; $F_{(6, 73)} = 1.951$; NS).

Recognition memory. As i.c.v. injection of soluble Aβ peptides in mice leads to impairment in the NOR test, recognition memory was evaluated in a paradigm similar to that performed for 5XFAD mice (see Materials and Methods). The test was performed 16 d after i.c.v. injection of either vehicle or soluble Aβ peptides. During training session (Fig. 6A), two-way repeated-measures ANOVA revealed neither an object effect ($F_{(1, 61)} = 3.774$; NS) nor a treatment effect ($F_{(6, 61)} = 0.8869$; NS) but a good matching of the measures ($F_{(61, 61)} = 2.288$; $p < 0.05$) and no treatment x object interaction ($F_{(6, 61)} = 1.574$; NS). During test session (Fig. 6B), two-way repeated-measures ANOVA revealed a clear object effect ($F_{(1, 61)} = 172.6$; $p < 0.05$), no treatment effect ($F_{(6, 61)} = 0.7804$; NS), a good matching of the measures ($F_{(61, 61)} = 3.686$; $p < 0.05$) and a treatment x object interaction ($F_{(6, 61)} = 5.642$; $p < 0.05$). Pairwise multiple comparisons demonstrated that the presence of donecopride (at all doses) resulted in the inhibition of soluble Aβ peptides-induced impairment of recognition memory (Fig. 6B). This was confirmed by discrimination index values showing that the memory impairment of the soluble Aβ group was reversed by donecopride treatment (one-way ANOVA, $F_{(6, 61)} = 0.622$; $p < 0.05$; Fig. 6C). The total exploration time was similar between the groups (one-way ANOVA, $F_{(6, 61)} = 0.7804$; NS; Fig. 6D).

This battery of behavioral tests demonstrated the ability of donecopride to protect mice from soluble Aβ peptides-induced toxicity. Notably, donecopride proved its efficiency when administered p.o. in this series of experiments. Moreover, donecopride at a dose of 3/mg/kg/d improved learning, even in the presence of soluble Aβ peptides.

Donecopride Displays in Cellulo Neuroprotective Activities and Reduces Tau Hyperphosphorylation in Rat Hippocampal Neuronal Cultures. Studies on the toxic role of Aβ have now shifted from insoluble fibrils to smaller, soluble peptides aggregates. Aβ peptides are produced as soluble monomers and undergo oligomerization and amyloid fibril formation via a nucleation-dependent polymerization process (Hartley and Lashue, 2010). During the course of in vitro Aβ fibril formation, various nonfibrillar intermediary aggregates are formed; collectively called "soluble oligomers and protofibrils", they have been shown to precede the appearance of fibrils. Increasing evidence from various sources points to soluble Aβ peptides/protofibrils as putative toxic species in AD pathogenesis (Sakono and Zako, 2010). By generating a solution of soluble Aβ peptides and adjusting its concentration and neuron exposure time, investigators reproduced early effects (oxidative stress) on neurons and long-term development of structural alterations (neuronal death) (Callizot *et al.*, 2013).

The effects of donecopride on neuronal survival, the neurite network, and tau phosphorylation were investigated in rat primary hippocampal neurons injured with soluble Aβ peptides (24-h exposure), donepezil being used as reference test compound.

Neuronal survival. An important loss of neurons stained with microtubule-associated protein 2 antibody was consecutive to the application of the soluble Aβ peptides (Fig. 7A, D). Donepezil, used here as a positive control, significantly protected neurons from death. Two doses of donecopride (100 nM and 500 nM) exerted neuroprotective effects to a similar extent as occurred with donepezil. However, the highest dose of donecopride was toxic, as the average survival was significantly lower than that observed in the soluble Aβ peptides condition (one-way ANOVA, $F_{(9, 48)} = 20{,}12$; $p < 0.05$), . The loss of the neuroprotective effect at 1 µM could be explained by the desensitization of 5-HT_4R challenged with high doses of agonists (Ansanay *et al.*, 1992; Barthet *et al.*, 2005). Such a bell-shaped curve was seen in another model of primary neuronal culture exposed to increasing doses of a 5-HT_4 agonist (Cho and Hu, 2007).

Neurite network. The total neurite network severely shrank on soluble Aβ peptides injury (Fig. 7B, D), but donepezil significantly preserved almost all of this network. Four doses

of donecopride (50 nM, 100 nM, 500 nM, and 1 μM) also exerted protective effects on the neurite network (one-way ANOVA, $F_{(9, 46)} = 28,84$; $p < 0.05$).

Tau phosphorylation. Hyperphosphorylation of tau detected with the AT100 antibody was observed under application of soluble Aβ peptides (Fig. 7C, D), but donepezil significantly mitigated this hyperphosphorylation. Similarly, donecopride (50 nM, 100 nM, 500 nM) significantly reduced the hyperphosphorylation of tau in a dose-dependent manner (one-way ANOVA, $F_{(9, 42)} = 18,05$; $p < 0.05$). Once again, this effect was lost with a higher concentration of donecopride. This may suggest that 5-HT_4R activation was involved in the decrease of tau phosphorylation and that the endocytosis of the receptor could be responsible for the loss of this effect at 1 μM.

Donecopride Preserves the Number of Synapses *in Cellulo* and Promotes the Formation of New Synapses in Neuronal Culture or Cultures of Rat Hippocampal Neurons. To investigate the formation of synapses, we assessed the distribution of presynaptic (synaptophysin) and postsynaptic markers [postsynaptic density protein 95 (PSD-95)] (Fig. 8A, B). A structure that tested positive for both PSD-95 and synaptophysin staining was considered a synapse. The stress resulting from the application of soluble Aβ peptides caused a reduction in the number of synapses (as previously shown by (Callizot *et al.*; 2013). Donepezil mitigated the loss of synapses. Similarly, donecopride also preserved the number of synapses in a dose-dependent manner from 5 nM to 1μM (one-way ANOVA, $F_{(9, 42)} = 5.585$, $p < 0.05$).

Because of the injury caused by the soluble Aβ peptides, the number of neurons was reduced in the experimental conditions, which led to a reduction in the number of synapses. Therefore, to estimate the number of synapses per neuron, we normalized the number of synapses by using the number of neurons in each condition. This adjustment showed that only donecopride significantly promoted the formation of new synapses, whereas donepezil had no effect (one-way ANOVA, $F_{(3,17)} = 1.788$, $p < 0.05$; Fig. 8B, C).

Discussion

The anti-amnesic properties previously displayed by donecopride toward the reversion of scopolamine-induced memory impairments in NMRI mice were confirmed after its chronic administration in two different animal models of AD. In transgenic 5XFAD mice, 3-mo i.p. administration of donecopride (1 mg/kg, twice a week) prevented the long-term mnesic

impairments observed in the NOR test in non-treated mice (Fig. 2). This effect is similar to one that we previously reported with the reference 5-HT_4R agonist, RS 67333, at the same dose of 1 mg/kg (Giannoni *et al.*, 2013; Baranger *et al.*, 2017). The use of the lowest active dose of donecopride and a twice a week administration protocol appear efficient to maintain the action of the compound and avoid the desensitization of the 5-HT_4R that has been reported in long-term administration of fluoxetine (Vidal *et al.*, 2009).

In a second mouse model of AD in which mice had a mnesic deficit after i.c.v. administration of soluble Aβ peptides, donecopride was orally administered for 18 d. The results confirmed the effect of donecopride in preventing recognition memory impairments that non-treated animals showed in a NOR test in a dose-dependent manner from 1 to 9 mg/kg (Fig. 6). This activity is comparable to that shown by donepezil in the same conditions. In the same model, donecopride (3 mg/kg) also prevented deficits in spatial working memory, a component of short-term memory, as shown in the Y-maze test (Fig. 4A), and in spatial reference memory, as tested in the MWM task. In the latter task, the effect of donecopride concerned both the improvement of learning capacities in mice, especially at a dose of 3 mg/kg (Fig. 5A), and of long-term memory performances at a dose of 1 mg/kg (Fig. 5D-E). These effects are again similar or even better to those observed with donepezil in the same conditions.

On the other hand, the chronic administration of donecopride in 5XFAD mice was accompanied by a decrease in amyloid load in soluble and insoluble brain fractions (Fig. 1). We postulate that donecopride decreased the production of Aβ through the non-amyloidogenic cleavage of APP and the consequent promotion of the sAPPα production, we previously demonstrated both *in vitro* (Lecoutey et al., 2014) and *in vivo* (Rochais et al., 2015). This anti-amyloid effect also resulted in a decrease in the number of amyloid plaques, as measured in the frontal and entorhinal cortex, but not in the hippocampus. The entorhinal cortex also showed a decrease in astrogliosis, which was not significant in the other brain areas (Fig. 3). We have previously reported that in this mouse model, because of the intense amyloid production, treatment with 5-HT_4R agonists should be initiated at the very early stages (4 wk old) to decrease the Aβ load and neuroinflammation in the hippocampus (Giannoni *et al.*, 2013).

Interestingly, we demonstrated here for the first time that the other main molecular cause implicated in the pathogenesis of AD appeared to be likewise affected by donecopride, since this compound decreased the phosphorylation status of tau in a dose-dependent manner starting at 50 nM in a cellular model of rat hippocampal neurons injured with AβO (Fig. 7C, D).

From a cellular mechanism point of view, donecopride appeared to display a neuroprotective role, as illustrated by the preservation of the number of neurons and synapses and the integrity of the neurite network (Fig. 7A, B, D and 8A, B). Beyond protection, donecopride seemed to exert a genuine neurotrophic effect by favoring the formation of new synapses (Fig. 8C), which is not observed with donepezil. This property, which may be linked to the promotion of learning, could be of extreme interest to patients with AD who face the loss of neurons by exerting a positive effect that is not achieved with donepezil, the current medication for treatment of AD.

Finally, this work provides a proof of concept that chronic administration of donecopride targets both AChE (its catalytic and peripheral sites) and 5-HT_4R, resulting in the alleviation of two major hallmarks of AD, amyloid aggregation and tau hyperphosphorylation. This targeting leads to neuroprotective and neurotrophic cellular consequences, which ultimately correlate with a clear improvement in working and long-term (recognition and spatial) memory capacities. We conclude that donecopride, or other compounds exhibiting similar Swiss army knife pleiotropic profiles, may on the one hand exert symptomatic sustained therapeutic effects through the restoration of cholinergic neurotransmission and, on the other, provide disease-modifying effects through its neurotrophic properties. As a result of these beneficial actions, even partial recovery of cognitive deficits in Alzheimer's patients could highly alleviate both the heavy health care cost and the social impact on families and caregivers. These challenges will soon be tested in clinical trials.

Figure legends

Fig. 1. Effects of donecopride on amyloid load after 3 mo of chronic treatment in soluble (A) and insoluble (B) fractions of 5XFAD mice brains. Results are expressed as mean ± SEM. Sample sizes: Soluble species: Vehicle (V)-Aβ_{40}: $n = 7$; Donecopride (D)-Aβ_{40}: $n = 7$; V-Aβ_{42}: $n = 6$; D-Aβ_{42}: $n = 7$. Insoluble species: V-Aβ_{40}: $n = 7$; D-Aβ_{40}: $n = 7$; V-Aβ_{42}: $n = 7$; D-Aβ_{42}: $n = 6$. Our aim was to have n = 7 mice in each group, but technical issues meant we were unable to obtain proper Aβ_{42} quantification from two mice. *$p < 0.05$ (unpaired Student's t test).

Fig. 2. Effects of donecopride on long-term memory performance after 3 mo of chronic treatment in 5XFAD mice. NOR test with 5-min exploration sessions and a 24-h intersession interval. Time spent by mice exploring left and right objects during training session (A) or familiar and novel objects during test session (B). *$p < 0.05$ vs. familiar object (two-way

repeated-measures ANOVA with object and treatment as factors, followed by Bonferroni's test). (C) Discrimination index calculated by using exploration times in test session and formula [(novel – familiar)]/(familiar + novel)]. Indices different from zero: *$p < 0.05$ (One sample Student's *t* test). (D) Total exploration time in test session was not significantly different among groups (unpaired Student's *t* test). (A-D) Data are expressed as mean ± SEM; $n = 7$ mice/group.

Fig. 3. Effects of donecopride on amyloid plaque load (A-D) and astrogliosis (E-H) after 3 mo of chronic treatment in 5XFAD mice. Brain slices were stained with thioflavin S (A-D) or an antibody directed against GFAP, a marker of astrocyte reactivity (E-H). Quantification of amyloid plaques or GFAP staining in frontal cortex (A, E), hippocampus (B, F), and entorhinal cortex (C, G) of mice treated with donecopride (1 mg/kg, twice a week for 3 mo) vs. mice that received vehicle. Analysis of thioflavin S or GFAP staining was performed blindly; data are presented as the mean number of plaques per mm^2 or LOG of the percentage of fraction area covered by GFAP staining in two to three tissue sections from the same brain area/animal (FIJI software). Each dot represents one mouse ($n = 7$ mice/group); horizontal lines show means ± SEM of each group. *$p < 0.05$ compared with vehicle (unpaired Student's *t* test, log-transformed data of GFAP staining are Gaussian distributed). Representative images of thioflavin S staining of amyloid plaques (D) or GFAP staining of astrocytes (H) in entorhinal cortex of 5XFAD mice treated with vehicle or donecopride. Prh, perirhinal cortex; DIEnt, dorsal intermediate entorhinal field; vSub, ventral subiculum; Thio S, thioflavin S.

Fig. 4. Effects of test items on spatial working memory in the Y-maze test. Mice were administered with increasing doses of compounds as described in the experimental procedures. Four days following i.c.v. infusion of either vehicle or soluble Aβ peptides, spontaneous alternation behavior (A) and arm entries (B) were recorded in the Y-maze test during a 5-min trial. Data are presented as mean alternation behavior (%) or mean of number of arm entries ± SEM. $n = 12$ mice/group, excepted in the [donecopride (9 mg/kg)] group in which one mouse did not move. *$p < 0.05$ (* different from vehicle control mice, # different from soluble Aβ peptides-injected mice, one-way ANOVA followed by Bonferroni's test). DPZ, donepezil.

Fig. 5. Effects of test items on learning capacities (A-C) and long-term memory (D-F) in the MWM test. Mice were administered with increasing doses of compounds as described in the experimental procedures. (A-C) From day +7 to day +11 following i.c.v. injection of vehicle or

soluble Aβ peptides, animals were trained to localize a hidden platform by using visual cues. The mean escape latency (A), mean swimming speed (B) and mean distance travelled (C) of four trials per day is presented for each group ± SEM (n = 12 mice/group). The probe test was performed 2 d after the last training session by removing the platform. The latency to target (i.e., time to perform the first cross over the former platform position) (C), the number of crossings over the former platform position (D) and the time in target quadrant (F) were determined. Data are presented as means ± SEM. Sample sizes: Vehicle, soluble Aβ, DPZ and donecopride (3mg/kg + Aβ): n = 12 mice/group; donecopride (1 and 9 mg/kg + Aβ): n = 11 mice/group; donecopride (9 mg/kg + vehicle): n = 10 mice. Floating mice were excluded from the analysis. *$p < 0.05$, (* different from vehicle control mice, # different from soluble Aβ peptides-injected mice, one-way ANOVA followed by Bonferoni's test). DPZ, donepezil.

Fig. 6. Effects of test items on soluble Aβ peptides-induced cognitive deficits in the NOR test. C57/Bl6J mice were i.c.v. injected at day 0 as described in the Materials and Methods. After habituation trials performed 15 d after i.c.v. injection, mice were subjected to a NOR test at day +16 with 5-min exploration sessions and 5-min intersession intervals. Time spent by mice exploring left and right objects during training session (A) or familiar and novel objects during test session (B). *$p < 0.05$ vs. familiar object; n.s., not significant (two-way repeated-measures ANOVA with object and treatment as factors, followed by Bonferroni's test). (C) Discrimination index calculated by using exploration times in test session and formula [(novel – familiar)]/(familiar + novel)]. Indices different from zero: *$p < 0.05$ (One sample Student's t test). Different from soluble Aβ peptides-injected mice: #$p < 0.05$ (one-way ANOVA followed by Bonferroni's test). DPZ, donepezil. (A-D) Data are mean ± SEM. The experiment was performed with n = 12 mice/groups. Mice with total time exploration of less than 5 sec in test session were excluded. Sample sizes: donecopride (1 mg/kg): n = 11 mice; vehicle and donecopride (9 mg/kg + vehicle and 9 mg/kg + Aβ): n = 10 mice/group; Soluble Aβ, DPZ and donecopride (3 mg/kg): n = 9 mice/group.

Fig. 7. Effects of test items after treatment with soluble Aβ peptides in a primary culture of hippocampal neurons. Effects on survival of microtubule-associated protein 2 (MAP-2) neurons (A), neurite network (B), and phosphorylation of tau (AT100) (C) in MAP-2 neurons. Donepezil (DPZ) served as a positive control. Results are expressed as mean ± SEM as a percentage of mean control. *$P < 0.05$ vs. Soluble Aβ peptides condition (one-way ANOVA

followed by PLSD Fisher's test). (D) Representative images of MAP-2 (red) and AT100 (green) staining of rat primary hippocampal neurons in the presence of vehicle, soluble Aβ peptides (20 µM), DPZ (1 µM), or donecopride (500 nM). Sample sizes: MAP-2 neurons: n = 6/group except for donecopride (100 nM and 1 µM) where n = 5/group; neurite network: n = 6/group except for DPZ and donecopride (1, 50, and 100 nM) were n = 5/group; tau Phosphorylation: n = 5/group except for DPZ and donecopride 50 nM where n = 6/group. Our aim was to obtain n = 6/group, however some cultures were not viable.

Fig. 8. Donecopride protect synapses after treatment with soluble Aβ peptides in a primary culture of hippocampal neurons. Effect of donecopride on total number of synapses (A) and on number of synapses per neuron (C). Donepezil (DPZ) served as a positive control. Results are expressed as mean ± SEM as a percentage of mean control. *$p < 0.05$ vs. Soluble Aβ peptides condition (one-way ANOVA followed by PLSD Fisher's test). (B) Representative images of synaptophysin (red), PSD95 (green), and Hoechst (blue) staining of rat primary hippocampal neurons in the presence of vehicle, soluble Aβ peptides (20 µM), DPZ (1 µM), or donecopride (500 nM). Sample sizes: synapse number: n = 5/group except for soluble Aβ and donecopride 50 nM where n = 6/group; synapse/neuron: n = 5/group except for soluble Aβ where n = 6/group. Our aim was to obtain n = 6/group, however some cultures were not viable.

Funding

This work was supported by funding from Normandie Valorisation, Normandie Incubation, and BPI France (AAP Maturation Preclinicalz); the French Agence Nationale de la Recherche (project MALAD ANR-12-JS007-0012-01, project ADAMGUARD ANR-12-BSV4-008-01 and project MAD5 ANR-15-CE16-0006); and The Fondation Vaincre Alzheimer (grant number #12721). K.B. was granted a research associate fellowship (Management of Talents) by the Excellence Initiative of Aix-Marseille University - A*MIDEX, a French "Programme Investissements d'Avenir."

Competing interests

The authors report no competing interests.

Declaration of transparency and scientific rigour

This Declaration acknowledges that this paper adheres to the principles for transparent reporting and scientific rigour of preclinical research as stated in the BJP guidelines for Design &

Analysis, Immunoblotting and Immunochemistry, and Animal Experimentation, and as recommended by funding agencies, publishers and other organisations engaged with supporting research.

References

Albasser MM, Davies M, Futter JE, Aggleton JP. Magnitude of the object recognition deficit associated with perirhinal cortex damage in rats: Effects of varying the lesion extent and the duration of the sample period. Behav Neurosci 2009; 123:115-124.

Alexander SP, Christopoulos A, Davenport AP, Kelly E, Marrion NV, Peters JA, *et al.* (2017). THE CONCISE GUIDE TO PHARMACOLOGY 2017/18: G protein-coupled receptors. Br J Pharmacol 174: Suppl 1:S17-S129.

Alexander SPH, Roberts RE, Broughton BRS, Sobey CG, George CH, Stanford SC, *et al.* (2018). Goals and practicalities of immunoblotting and immunohistochemistry: A guide for submission to the British Journal of Pharmacology. Br J Pharmacol 175: 407-411.

Ansanay H, Sebben M, Bockaert J, Dumuis A. Characterization of homologous 5-hydroxytryptamine4 receptor desensitization in colliculi neurons. Mol Pharmacol 1992; 42:808-816.

Baranger K, *et al.* Chronic treatments with a 5-HT_4 receptor agonist decrease amyloid pathology in the entorhinal cortex and learning and memory deficits in the 5xFAD mouse model of Alzheimer's disease. Neuropharmacology 2017; 126:128-141.

Barthet G, *et al.* Uncoupling and endocytosis of 5-hydroxytryptamine 4 receptors: distinct molecular events with different GRK2 requirements. J Biol Chem 2005; 280:27924-27934.

Bartsch T, *et al.* Focal lesions of human hippocampal CA1 neurons in transient global amnesia impair place memory. Science 2010; 328:1412-1415.

Benjamin MJ, Cifelli A, Garrard P, Caine D, Jones FW The role of working memory and verbal fluency in autobiographical memory in early Alzheimer's disease and matched controls. Neuropsychologia 2015; 78:115-121.

Bianchini F, *et al.* A selective egocentric topographical working memory deficit in the early stages of Alzheimer's disease: a preliminary study. Am J Alzheimers Dis Other Demen 2014; 29:749-754.

Bouter Y, *et al.* N-truncated amyloid beta (Abeta) 4-42 forms stable aggregates and induces acute and long-lasting behavioral deficits. Acta Neuropathol 2013; 126:189-205.

Broadbent NJ, Squire LR, Clark RE. Reversible hippocampal lesions disrupt water maze performance during both recent and remote memory tests. Learn Mem 2006; 13:187-191.

Brown MW, Barker GR, Aggleton JP, Warburton EC. What pharmacological interventions indicate concerning the role of the perirhinal cortex in recognition memory. Neuropsychologia 2012; 50:3122-3140.

Callizot N, Combes M, Steinschneider R, Poindron P. Operational dissection of beta-amyloid cytopathic effects on cultured neurons. J Neurosci Res 2013; 91:706-716.

Cavalli A, *et al.* Multi-target-directed ligands to combat neurodegenerative diseases. J Med Chem 2008; 51:347-372.

Cho S, Hu Y. Activation of 5-HT_4 receptors inhibits secretion of beta-amyloid peptides and increases neuronal survival. Exp Neurol 2007; 203:274-278.

Citron M. Alzheimer's disease: strategies for disease modification. Nat Rev Drug Discov 2010; 9:387-398.

Curtis MJ, Alexander S, Cirino G, Docherty JR, George CH, Giembycz MA, *et al.* (2018). Experimental design and analysis and their reporting II: updated and simplified guidance for authors and peer reviewers. Br J Pharmacol 175: 987-993.

Crouzin N, *et al.* Area-specific alterations of synaptic plasticity in the 5XFAD mouse model of Alzheimer's disease: dissociation between somatosensory cortex and hippocampus. PLoS One 2013; 8:e74667.

deToledo-Morrell L, *et al.* MRI-derived entorhinal volume is a good predictor of conversion from MCI to AD. Neurobiol Aging 2004; 25:1197-1203.

Desbene C, *et al.* Critical role of cPLA2 in Abeta oligomer-induced neurodegeneration and memory deficit. Neurobiol Aging 2012; 33:1123 e1117-1129.

Freret T, Billard JM, Schumann-Bard P, Dutar P, Dauphin F, Boulouard M, *et al.* (2012). Rescue of cognitive aging by long-lasting environmental enrichment exposure initiated before median lifespan. Neurobiol Aging 33: 1005 e1001-1010.

Freret T, Lelong-Boulouard V, Lecouflet P, Hamidouche K, Dauphin F, & Boulouard M (2017). Co-modulation of an allosteric modulator of nicotinic receptor-cholinesterase inhibitor (galantamine) and a 5-HT4 receptor agonist (RS-67333): effect on scopolamine-induced memory deficit in the mouse. Psychopharmacology (Berl) 234: 2365-2374.

Frolich L, *et al.* Open-label, multicenter, phase III extension study of idalopirdine as adjunctive to donepezil for the treatment of mild-moderate Alzheimer's disease. J Alzheimers Dis 2019; 67:303-313.

Garcia P, *et al.* Ciliary neurotrophic factor cell-based delivery prevents synaptic impairment and improves memory in mouse models of Alzheimer's disease. J Neurosci 2010; 30:7516-7527.

Giannoni P, *et al.* Early administration of RS 67333, a specific 5-HT4 receptor agonist, prevents amyloidogenesis and behavioral deficits in the 5XFAD mouse model of Alzheimer's disease. Front Aging Neurosci 2013; 5:96.

Giannoni P, *et al.* Cerebrovascular pathology during the progression of experimental Alzheimer's disease. Neurobiol Dis 2016; 88:107-117.

Girard SD, *et al.* Onset of hippocampus-dependent memory impairments in 5XFAD transgenic mouse model of Alzheimer's disease. Hippocampus 2014; 24:762-772.

Goodrich-Hunsaker NJ, Livingstone SA, Skelton RW, Hopkins RO. Spatial deficits in a virtual water maze in amnesic participants with hippocampal damage. Hippocampus 2010; 20:481-491.

Harding SD, Sharman JL, Faccenda E, Southan C, Pawson AJ, Ireland S *et al.* (2018). The IUPHAR/BPS Guide to PHARMACOLOGY in 2018: updates and expansion to encompass the new guide to IMMUNOPHARMACOLOGY. Nucl Acids Res 46: D1091-D1106.

Inestrosa NC, *et al.* Acetylcholinesterase accelerates assembly of amyloid-beta-peptides into Alzheimer's fibrils: possible role of the peripheral site of the enzyme. Neuron 1996; 16:881-891.

Jan A, Hartley DM, Lashuel HA. Preparation and characterization of toxic Abeta aggregates for structural and functional studies in Alzheimer's disease research. Nat Protoc 2010; 5:1186-1209.

Kilbinger H, Wolf D. Effects of 5-HT_4 receptor stimulation on basal and electrically evoked release of acetylcholine from guinea-pig myenteric plexus. Naunyn-Schmiedeberg's Arch Pharmacol 1992; 345:270-275.

Kriem B, *et al.* Cytosolic phospholipase A2 mediates neuronal apoptosis induced by soluble oligomers of the amyloid-beta peptide. FASEB J 2005; 19:85-87.

Lagun D, Manzanares C, Zola SM, Buffalo EA, Agichtein E. Detecting cognitive impairment by eye movement analysis using automatic classification algorithms. J Neurosci Methods 2011; 201:196-203.

Lecoutey C, *et al.* Design of donecopride, a dual serotonin subtype 4 receptor agonist/acetylcholinesterase inhibitor with potential interest for Alzheimer's disease treatment. Proc Natl Acad Sci USA 2014; 111:E3825-3830.

Leger M, Quiedeville A, Bouet V, Haelewyn B, Boulouard M, Schumann-Bard P, *et al.* (2013). Object recognition test in mice. Nat Protoc 8: 2531-2537.

Maillet M, *et al.* Crosstalk between Rap1 and Rac regulates secretion of sAPPalpha. Nat Cell Biol 2003; 5:633-639.

Malaplate-Armand C, *et al.* Soluble oligomers of amyloid-beta peptide induce neuronal apoptosis by activating a cPLA2-dependent sphingomyelinase-ceramide pathway. Neurobiol Dis 2006; 23:178-189.

Martin SJ, de Hoz L, Morris RG. Retrograde amnesia: neither partial nor complete hippocampal lesions in rats result in preferential sparing of remote spatial memory, even after reminding. Neuropsychologia 2005; 43:609-624.

Melnikova I. Therapies for Alzheimer's disease. Nat Rev Drug Discov 2007; 6:341-342.

Rosini M, Simoni E, Minarini A, Melchiorre C. Multi-target design strategies in the context of Alzheimer's disease: acetylcholinesterase inhibition and NMDA receptor antagonism as the driving forces. Neurochem Res 2014; 39:1914-1923.

Musial A, Bajda M, Malawska B. Recent developments in cholinesterases inhibitors for Alzheimer's disease treatment. Curr Med Chem 2007; 14:2654-2679.

Mumby DG, Astur RS, Weisend MP, Sutherland RJ. Retrograde amnesia and selective damage to the hippocampal formation: memory for places and object discriminations. Behav Brain Res 1999; 106(1-2):97-107.

Norman G, Eacott MJ. Dissociable effects of lesions to the perirhinal cortex and the postrhinal cortex on memory for context and objects in rats. Behav Neurosci 2005; 119:557-566.

Oakley H, *et al.* Intraneuronal beta-amyloid aggregates, neurodegeneration, and neuron loss in transgenic mice with five familial Alzheimer's disease mutations: potential factors in amyloid plaque formation. J Neurosci 2006; 26:10129-10140.

Pillot T, *et al.* The nonfibrillar amyloid beta-peptide induces apoptotic neuronal cell death: involvement of its C-terminal fusogenic domain. J Neurochem 1999; 73:1626-1634.

Rochais C, *et al.* Novel multitarget-directed ligands (MTDLs) with acetylcholinesterase (AChE) inhibitory and serotonergic subtype 4 receptor (5-HT_4R) agonist activities as potential agents against Alzheimer's disease: the design of donecopride. J Med Chem 2015; 58:3172-3187.

Sakono M, Zako T. Amyloid oligomers: formation and toxicity of Abeta oligomers. FEBS J 2010; 277:1348-1358.

Sarter M, Schneider HH, Stephens DN. Treatment strategies for senile dementia: antagonist beta-carbolines. Trends Neurosci 1988; 11:13-17.

Schmitt B, Bernhardt T, Moeller HJ, Heuser I, Frolich L. Combination therapy in Alzheimer's disease: a review of current evidence. CNS Drugs 2004; 18:827-844.

Schroeter ML, *et al.* Executive deficits are related to the inferior frontal junction in early dementia. Brain 2012; 135(Pt 1):201-215.

Spellman T, *et al.* Hippocampal-prefrontal input supports spatial encoding in working memory. Nature 2015; 522:309-314.

Stoub TR, *et al.* MRI predictors of risk of incident Alzheimer disease: a longitudinal study. Neurology 2005; 64:1520-1524.

Taylor KI, Probst A, Miserez AR, Monsch AU, Tolnay M. Clinical course of neuropathologically confirmed frontal-variant Alzheimer's disease. Nat Clin Pract Neurol 2008; 4:226-232.

Vidal R, Valdizan EM, Mostany R, Pazos A, & Castro E (2009). Long-term treatment with fluoxetine induces desensitization of 5-HT4 receptor-dependent signalling and functionality in rat brain. J Neurochem 110: 1120-1127.

Wallace TL, Ballard TM, Glavis-Bloom C. Animal paradigms to assess cognition with translation to humans. Handb Exp Pharmacol 2015; 228:27-57.

Watson HC, Lee AC. The perirhinal cortex and recognition memory interference. J Neurosci 2013; 33:4192-4200.

Wang H, Zhang H. Reconsideration of anticholinesterase therapeutic strategies against Alzheimer's disease. ACS Chem Neurosci 2019; 10 (2):852–862 doi:10.1021/acschemneuro.8b00391.

Yoon T, Okada J, Jung MW, Kim JJ. Prefrontal cortex and hippocampus subserve different components of working memory in rats. Learn Mem 2008; 15:97-105.

Youssef I, *et al.* N-truncated amyloid-beta oligomers induce learning impairment and neuronal apoptosis. Neurobiol Aging 2008; 29:1319-1333.

Zeamer A, Richardson RL, Weiss AR, Bachevalier J. The development of object recognition memory in rhesus macaques with neonatal lesions of the perirhinal cortex. Dev Cogn Neurosci 2015; 11:31-41.

Zola SM, Manzanares CM, Clopton P, Lah JJ, Levey AI. A behavioral task predicts conversion to mild cognitive impairment and Alzheimer's disease. Am J Alzheimers Dis Other Demen 2013; 28:179-184.

Donecopride, a Swiss army knife with potential interest against Alzheimer's disease

Running title: **Donecopride, a Swiss army knife against AD**

Christophe Rochais[a,b], Cédric Lecoutey[a,b], Katia Hamidouche[a,c], Patrizia Giannoni[d,1], Florence Gaven[d,2], Eleazere Cem[d], Kevin Baranger[e], Thomas Freret[a,c], Joël Bockaert[d], Santiago Rivera[e], Michel Boulouard[a,c], Patrick Dallemagne[a,b,3], Sylvie Claeysen[d,3]

[a]Normandie Univ, F-14032 Caen, France; [b]UNICAEN, CERMN (Centre d'Etudes et de Recherche sur le Médicament de Normandie), F-14032 Caen, France; [c]UNICAEN, INSERM U1075 COMETE F-14032 Caen, France; [d]IGF, University of Montpellier, CNRS, INSERM, F-34094, Montpellier, France; [e]Aix-Marseille University, CNRS, INP, Inst Neurophysiopathol, F-13344, Marseille, France

[1]Present address: Equipe Chrome, EA7352, Université de Nîmes, F-30000 Nîmes, France.
[2]Present address: CRBM, CNRS UMR5237, F-34293 Montpellier cedex 5, France.
[3]P.D. and S. C. contributed equally to this work.

Corresponding authors:
Patrick Dallemagne
CERMN – EA4258
Boulevard Becquerel, 14032 Caen, France
+33 231 566 813
Email: patrick.dallemagne@unicaen.fr

Sylvie Claeysen
IGF – CNRS UMR5203 – INSERM U1191 – Univ. Montpellier
141 rue de la Cardonille, 34094 Montpellier cedex 5, France
+33 434 359 215
Email: sylvie.claeysen@igf.cnrs.fr

SI Material and methods

Mice

All the experimental procedures were conducted in accordance with National and European regulations (EU directive N° 2010/63) and approved protocols (D13-055-08 and B54-547-28). All efforts were made to minimize animal suffering and to reduce the number of mice used. The generation of transgenic 5xFAD mice has been described previously (1). These mice carry mutations in both human amyloid precursor protein (APP_{695}) and presenilin-1 (*PSEN1)* genes. The *APP* gene harbors three Familial Alzheimer's Disease (FAD) mutations: Swedish (K670N, M671L), Florida (I716V), and London (V717I). The human *PSEN1* gene harbors two FAD mutations: M146L and L286V. Human gene expression is regulated by neural-specific elements of the mouse Thy1 promoter to drive neuronal specificity. The 5XFAD strain (B6/SJL genetic background) was maintained by crossing heterozygous transgenic mice with B6/SJL F1 breeders (Jackson Laboratories, Bar Harbor, Maine, USA). These mice were then derived in a C57BL/6 genetic background. F1 male mice resulting from crossing 5XFAD (B6/SJL) and C57BL/6 mice were then crossed with C57BL/6 females and the male offspring backcrossed more than eight times with C57BL/6 females as described in (2). Female 5XFAD heterozygous transgenic mice were used for the experiments (7 mice/group). Genomic DNA was extracted from mice tail tips to assess their genotype by PCR. All transgenic mice were bred in our animal facility. For soluble Aβ peptide treatments, C57Bl6/J male mice (3 months of age, 12 mice/group) were purchased from Janvier, France. All mice had access to food and water *ad libitum* and were housed under a 12 h light-dark cycle (12 h-12 h) at 22 ± 2°C.

Drugs

Donepezil (2,3-Dihydro-5,6-dimethoxy-2-[[1-(phenylmethyl)-4-piperidinyl]methyl]-1H-inden-1-one) was purchased from Tocris Bioscience (R&D Systems Europe, Lille, France). Donecopride (1-(4-amino-5-chloro-2-methoxyphenyl)-3-[1-(cyclohexylmethyl)-4-piperidinyl] propan-1-one) and its fumarate salt were synthesized as reported in (3). For ip administration, compounds were resuspended in DMSO (37.5 µg/µl, stored at -20°C) and freshly diluted 1:250 in 0.9% NaCl prior administration. Vehicle solution (0.9% NaCl, 0.4% DMSO) was used as control. For per os dosing, compounds were solubilized in 0.9% NaCl.

5XFAD experiments

Chronic treatments in 5XFAD mice

Two-month-old 5XFAD mice received either drugs (1 mg/kg) or vehicle solution i.p. twice a week for 3 months. At the end of the experiments, mice were anesthetized with a mixture of 100 mg/kg ketamine and 10 mg/kg xylazine in saline solution and perfused transcardially with PBS. Brains were quickly isolated on ice, the olfactory bulbs and cerebellum removed and the two hemispheres divided. One hemisphere (or microdissected areas) was frozen on dry ice and stored at -80°C for biochemical analysis, while the other was post-fixed in 4 % PFA for immunohistochemistry (IHC).

Brain extract preparation

Frontal cortex, hippocampus and entorhinal cortex of 5XFAD mice and controls were thawed, weighed and homogenized in 4 volumes of tris-saline (50 mM Tris-HCl pH = 7.4, 150 mM NaCl) with a protease inhibitor cocktail (Roche Applied Science, Meylan, France). The resulting homogenates were centrifuged at 54,000 x g for 20 minutes and supernatants (the "soluble fraction") collected and aliquoted for storage at -80°C. Pellets were resuspended by brief sonication in 10 volumes of 6 M guanidine HCl in 50 mM Tris-HCl, pH = 7.6 and centrifuged again at 26,500 x g for 20 minutes. Supernatants (the "insoluble fraction") were aliquoted and stored at -80°C (4).

Quantification of Aβ40 and Aβ42

ELISA kits from IBL International (Hamburg, Germany) for the dosage of $A\beta_{40}$ (human amyloid β (1-40) assay kit, #27713) or $A\beta_{42}$ (human amyloid β (1-42) assay kit, #27719) were used according to the manufacturer's instructions. Reactions were read at 620 nm and 450 nm using an Infinite 2000 luminescence counter. The obtained values were normalized to the protein concentration of each sample, measured using a BCA protein assay (Sigma-Aldrich).

Immunohistochemistry

Thirty-micrometer-thick sections were cut using a vibratome (Microm HM 650V, Thermo Scientific, Saint Herblain, France) and stored in cryoprotectant medium at -20°C. For the labeling of amyloid plaques, free-floating tissue sections of frontal cortex, hippocampus and entorhinal cortex (coordinates from the bregma: frontal cortex = 1.98 mm, hippocampus = -1.94 mm, entorhinal cortex = -3.08 mm) were extensively washed in PBS and then and mounted on gelatin-coated slides. After drying, slides were immersed for 10 min in a solution of thioflavin-S (1% in PBS, #T1892-25G, Sigma-Aldrich, St. Quentin Fallavier, France) and sequentially dehydrated in ethanol 70°, 80°, 95° and 100° (2 min each). Slices were immersed for 5 min in two solutions of xylene, and a non-aqueous mounting medium (EUKITT) was used before adding coverslips. For GFAP (glial fibrillary acidic protein) staining, free-floating brain sections were incubated in blocking solution (PBS; 3% BSA; 0.1% Triton X-100) for 1 h. Then the slices were incubated with polyclonal rabbit anti-GFAP (1:1000, Z0334, Dako, Les Ullis, France, RRID:AB_10013382) overnight at 4°C. A secondary Alexafluor 594 goat anti-rabbit antibody (1:1000, A11012, Life Technologies, Saint Aubin, France, RRID:AB_141359) was added for 2 h. All slices were finally mounted on poly-lysine slides and cover slipped.

Image acquisition and analysis

Images were acquired with an AxioImager Z1 microscope (Carl Zeiss S.A.S., Marly le Roi, France), and blindly analyzed using the FIJI software. Quantification of amyloid plaques (Thioflavin S staining, 10X objective) is represented as number of particles per mm^2 and averaged from two different measurements. Briefly, background was removed using the "Substract background" module of FIJI software with default set up (50 pixels), and the plugin Log3D (sigma X:3, sigma Y:3) with default threshold and Analyze particle function (0-Infinity) were used to count the plaques in the region of interest (ROI). The number of detected particles was divided by the size of the ROI in mm^2. GFAP-stained images (20X) were acquired maintaining constant exposure for all samples across single experiments. Quantification (area fractions) was averaged from two to three different measurements and results are expressed as percent of vehicle condition.

Novel object recognition test of 5XFAD mice

The cognitive performance of 5XFAD mice was tested after 3 month of treatment using the novel object recognition (NOR) test (5). Animals were extensively handled during drug treatment prior to the test onset. Each day, mice were allowed to familiarize with the test room for at least 1 h prior to the test. Testing was carried out in a Plexiglas box (width: 35 cm, length: 20 cm, height: 20 cm) placed in a dimly lit room (12-15 lux). On day 1 and 2, each mouse was habituated to the empty box for 10 min/day. On day 3, two objects (constructed out of plastic toys) were positioned in the cage, 5 cm away from the opposing walls. During the training session, each animal was placed between the two objects, facing the wall and then was allowed to explore the objects for 5 min. Mice were then returned to their home cage and 24 h later went through a 5 min test session in which one of the two (familiar) objects was replaced by a new one (novel). The whole experiment was video-recorded and object exploration [time spent by the mouse nose in contact with the object or by sniffing it at a distance ≤ 1 cm] was blindly measured. Two parameters were considered: 1) the exploration time (sec) spent by the animal interacting with the two familiar objects during the training session and 2) the exploration time spent by the animal interacting with the novel object relative to the total exploration time ([novel/(familiar + novel)] × 100) during the test. A discrimination index was also calculated ([novel − familiar]/[familiar + novel]).

Soluble Aβ peptides *in vivo* experiments

Preparation and stereotaxic injection of soluble Aβ peptides to C57BL/6 mice

$A\beta_{1-42}$ was obtained from Bachem (ref H1368) (batch number: 1052301). The preparation of stable soluble $A\beta_{1-42}$ peptides was performed according to (6). The peptides preparation contained a mixture of stable trimers and tetramers of $A\beta_{1-42}$, as well as monomeric forms of the peptide. All peptides preparations are characterized in terms of peptides composition and in vitro neurotoxicity.

Single intra-cerebroventricular injection of C57BL/6 mice with vehicle or soluble Aβ peptides: under anesthesia (ip injection of a mixture of ketamine/xylasine at a dose of 110 and 15 mg/kg, respectively), soluble Aβ peptides (1 µL) or vehicle (1 µL) were injected into the right lateral ventricle. Injections were made using 10 µL Hamilton micro syringes fitted with a 26-gauge needle. The procedure was terminated by a subcutaneous injection of metacam (analgesia) at a dose of 5 mg/kg. Animals were then placed

individually in their home-cage and the cage was placed in a heated cabinet until the animal has fully recovered. Animals were carefully monitored to control recovery after anesthesia.
Compound dosing (total volume of 200 µL) started one day before icv injection of soluble Aβ peptides and was done for 19 consecutive days. Behavioral tests were performed according to the time-schedule presented in Supplementary figure 1.

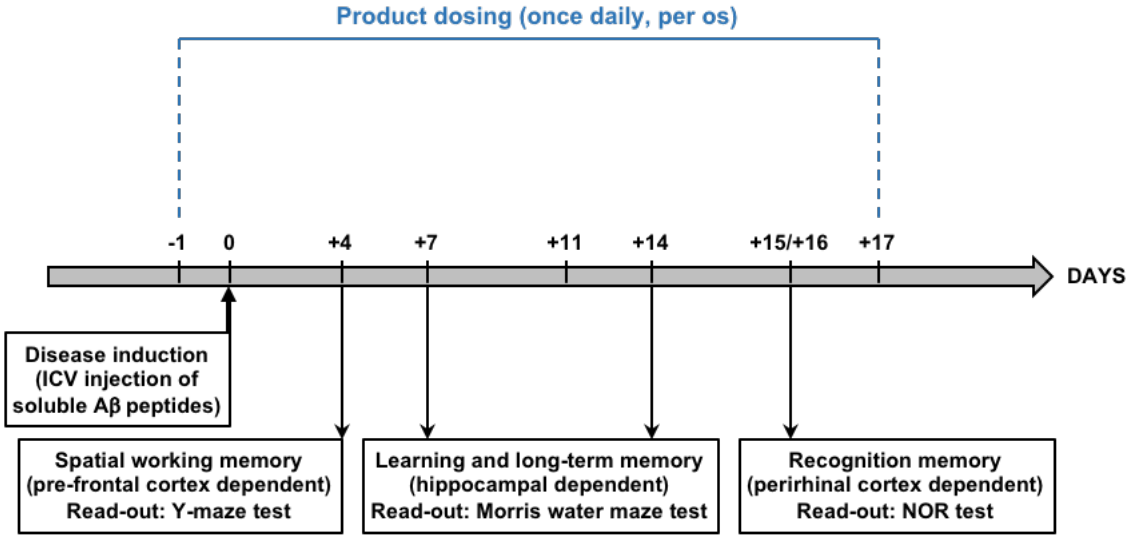

Supplementary figure 1: Overall organization and time-schedule of the soluble Aβ peptides *in vivo* experiments

Y-Maze test of C57BL/6 mice injected with soluble Aβ peptides
Behavioral tests were performed 1 h after dosing at day +4. Immediate spatial working memory performance was assessed by recording spontaneous alternation behavior in a Y-maze. The maze is made of opaque Plexiglas and each of the three arms is 40 cm long, 14 cm high, 10 cm wide and positioned at equal angles. The apparatus is placed in a homogeneously lit test room to obtain 12-15 lux in all arms as well as in the central zone. Mice are placed in the middle of one arm and allowed to explore the maze freely during 5 min session. The series of arm entries are video recorded (Smart v3.0 software, Bioseb) and an arm entry is considered complete when the hind paws of the mouse are completely placed in the arm. Alternation is defined as successive entries into the 3 arms on overlapping triplet sets. The percentage of alternation is calculated as the ratio of actual total alternations to possible alternations, defined as the number of arm entries minus 2, multiplied by 100. Locomotor activity is also recorded and evaluated during this phase (e.g. motivational index) by monitoring average speed and total distance.

Morris Water Maze (MWM) test of C57BL/6 mice injected with soluble Aβ peptides
Habituation trials (visible platform) - The MWM test is performed as described in (6). The experimental apparatus consists of a circular water tank (diameter = 100 cm; height = 50 cm) containing water at 21°C to a depth of 25 cm and rendered opaque to block the view past the water surface by adding an aqueous acrylic emulsion. A platform (diameter = 10 cm) is used and placed at the midpoint of a quadrant. The pool is located in a test room, homogeneously illuminated at 100 lux. The swimming path of the animals is recorded using a video tracking system. Mice are brought to the experimental room for at least 30 min prior to testing, to enable acclimation to the experimental room conditions. Navigation to a visible platform is carried out before place-navigation, to evaluate visual and motor abilities of all mice. Mice are submitted to 4 trials of 60 s per day (during 2 consecutive days), with an inter-trial interval of at least 1 h. Once mice have found the platform, they are left alone on the platform for an additional time of 30 s. There are no additional cues in the room. The platform position and starting points are randomly distributed over all 4 quadrants of the pool. Mice that fail to find the platform after 60 s are guided to its location and placed on the platform for 30 s.
Memory-acquisition trials (learning trials with hidden platform) are performed during 5 consecutive days and used to reach a steady state of escape latency. Mice are brought to the experimental room for at least 30 min prior to testing, to enable acclimation to the experimental room conditions. The hidden platform is submerged 1 cm below the water surface and placed at the midpoint of one quadrant. The

pool is located in a test room homogeneously illuminated at 100 lux and containing various prominent visual cues. The swimming paths, swimming distance, swimming speed and thigmotaxis are recorded using a video tracking system. Mice are submitted to 4 trials of 60 s per day, with an inter-trial interval of at least 1 h. The mice are allowed to swim freely for 60 s, left alone for an additional 30 s on the hidden platform and then returned to their home cage during the inter-trial interval. Start positions (set at the border of quadrants) are randomly selected for each animal. In each trial, the time required to escape onto the hidden platform is recorded. Mice that fail to find the platform after 60 s are guided to and placed onto the platform for 30 s, before they are returned to their home cage.
Memory-retention trials (probe trials, no platform) are performed two days after the last training session. Mice are again acclimated to the experimental room for at least 30 min prior to testing. The platform is removed and each animal is allowed a free 60 sec swim. During the trial, the time spent in the target quadrant, the time spend in the quadrant opposite, and the crossings over the former platform location are measured and monitored by video tracking.

NOR test of C57BL/6 mice injected with soluble Aβ peptides

Behavioral tests were performed 1 h after dosing at day +15/+16. One day before the cognitive test (i.e. at day +15), mice are habituated during a 10 minutes' trial during which they are placed in an empty open field (12-15 lux). The day of the cognitive test (i.e. day +16), animals are placed in the same open field and are allowed to explore freely two identical objects for a trial of five minutes (acquisition trial). Then the animals are returned in their home-cage for an inter-trial time of five minutes. During the retention trial, animals are allowed to explore two different objects: one familiar and one novel object. During this time, the experimenter, blind to the treatment, record the time the mouse is actively exploring each object. All trials are video recorded (Smart v3.0 software, Bioseb). A discrimination index is then generated: Discrimination index = (time exploring novel object – time exploring familiar object) / total exploration time.

Soluble Aβ peptides experiments on primary neuronal culture

Primary culture of hippocampal neurons

Rat hippocampal neurons were cultured as described in (7). Pregnant female rats of 17 days gestation (Rats Wistar; Janvier Labs France) were killed using a deep anesthesia with CO_2 chamber followed by a cervical dislocation. Then, fetuses were removed from the uterus and immediately placed in ice-cold L15 Leibovitz medium with a 2% penicillin (10,000 U/ml) and streptomycin (10 mg/ml) solution (PS) and 1% bovine serum albumin (BSA). Hippocampal neurons were treated for 20 min at 37°C with a trypsin-EDTA solution at a final concentration of 0.05% trypsin and 0.02% EDTA. The dissociation was stopped by adding Dulbecco's modified Eagle's medium (DMEM) with 4.5 g/liter of glucose, containing DNAse I grade II (final concentration 0.5 mg/ml) and 10% fetal calf serum (FCS). Cells were mechanically dissociated by three forced passages through the tip of a 10-ml pipette and then centrifuged at 515 x g for 10 min at 4°C. The supernatant was discarded, and the pellet was resuspended in a defined culture medium consisting of Neurobasal medium with a 2% solution of B27 supplement, 2 mmol/liter of L-glutamine, 2% of PS solution, and 10 ng/ml of brain-derived neurotrophic factor (BDNF). Viable cells were counted in a Neubauer cytometer, using the trypan blue exclusion test. Cells were seeded at a density of 20,000 per well in 96-well plates precoated with poly-L-lysine and cultured at 37°C in an air (95%)-CO_2 (5%) incubator. The medium was changed every 2 days.

Test compounds and human $A\beta_{1-42}$ exposure

The hippocampal neurons were exposed with Aβ solutions after 17 days of culture. The $A\beta_{1-42}$ preparation was done following the procedure described in (7).
Briefly, $A\beta_{1-42}$ peptide was dissolved in the defined culture medium mentioned above, at an initial concentration of 40 µM. This solution was gently agitated for 3 days at 37°C in the dark and immediately used after being properly diluted in culture medium to the concentrations used (20 µM (plate 1 for MAP2/Tau stainings) or 2.5 µM (plate 2 for PSD95/Synaptophysin stainings) corresponding to 2 µM or 0.25µM of soluble Aβ peptides respectively).
Donepezil (1µM) or Donecopride (1nM to 1µM) were solved in culture medium and preincubated 1 hour before Aβ application. $A\beta_{1-42}$ preparation was added to a final concentration of 20 or 2.5µM (= 2 µM or 0.25µM of soluble Aβ peptides, evaluated by automatic WB) diluted in control medium in presence of the compounds. The compounds were in a 96 well plate (6 wells per condition).

Survival, neurite network and phospho tau evaluation

24 hours after intoxication, the hippocampal neurons were fixed by a cold solution of ethanol (95%) and acetic acid (5%) for 5 min at -20°C. After permeabilization with 0.1% of saponin, cells will be incubated for 2 hours with 1/ a chicken polyclonal antibody anti microtubule-associated-protein 2 (MAP-2, RRID:AB_2138153), diluted at 1/1000 in PBS containing 1% fetal calf serum and 0.1% of saponin (this antibody allows the specific staining of neuronal cell bodies and neurites; and allow the study of neuronal cell death and neurite network) or 2/ a mouse monoclonal antibody anti-phospho Tau (AT100, RRID:AB_223652) at dilution of 1/400 in PBS containing 1% fetal calf serum and 0.1% of saponin. These antibodies were revealed with Alexa Fluor 488 goat anti mouse IgG (RRID:AB_2532075) and Alexa Fluor 568 goat anti-chicken IgG (SAB4600084, Sigma-Aldrich) at the dilution 1/400 in PBS containing 1% FCS, 0.1% saponin, for 1 hour at room temperature.
For each condition, 30 pictures (representative of the whole well area) per well were taken using ImageXpress (Molecular Devices, RRID:SCR_016654) at 20X magnification. All images were taken with the same acquisition parameters. Analyses were performed automatically by using Custom Module Editor (Molecular Devices). The following endpoints were assessed: total number of neurons (neuron survival, number of MAP-2 positive neurons), neurite network (in µm of MAP-2 positive neurons), area of tau in neurons (µm², overlapping with MAP-2 positive neurons).

Synapses evaluation

24 hours after intoxication, the hippocampal neurons were fixed by a cold solution of ethanol (95%) and acetic acid (5%) for 5 min at -20°C. After permeabilization with 0.1% of saponin, cells were incubated for 2 hours with: 1/ a mouse monoclonal antibody anti post synaptic density 95kDa (PSD95, RRID:AB_300453) at a dilution of 1/100 in PBS containing 1% fetal calf serum and 0.1% of saponin or 2/ a rabbit polyclonal antibody anti-synaptophysin (SYN, RRID:AB_306124) at the dilution of 1/100 in PBS containing 1% fetal calf serum and 0.1% of saponin. These antibodies were revealed with Alexa Fluor 488 goat anti mouse IgG and Alexa Fluor 568 goat anti-rabbit IgG at the dilution 1/400 in PBS containing 1% FCS, 0.1% saponin, for 1 hour at room temperature.
For each condition, 40 pictures per well were taken using ImageXpress (Molecular Devices) with 40x magnification. All images were taken with the same acquisition parameters.
Synapses evaluation were performed automatically by using Custom module editor (Molecular Devices). The total number of synapses (overlapping between PSD95/SYN) was then assessed.

References

1. Oakley H, et al. (2006) Intraneuronal beta-amyloid aggregates, neurodegeneration, and neuron loss in transgenic mice with five familial Alzheimer's disease mutations: potential factors in amyloid plaque formation. *J Neurosci* 26(40):10129-10140.
2. Baranger K, et al. (2016) MT5-MMP is a new pro-amyloidogenic proteinase that promotes amyloid pathology and cognitive decline in a transgenic mouse model of Alzheimer's disease. *Cell Mol Life Sci* 73(1):217-236.
3. Lecoutey C, et al. (2014) Design of donecopride, a dual serotonin subtype 4 receptor agonist/acetylcholinesterase inhibitor with potential interest for Alzheimer's disease treatment. *Proc Natl Acad Sci U S A* 111(36):E3825-3830.
4. Morishima-Kawashima M, et al. (2000) Effect of apolipoprotein E allele epsilon4 on the initial phase of amyloid beta-protein accumulation in the human brain. *Am J Pathol* 157(6):2093-2099.
5. Bevins RA & Besheer J (2006) Object recognition in rats and mice: a one-trial non-matching-to-sample learning task to study 'recognition memory'. *Nat Protoc* 1(3):1306-1311.
6. Garcia P, et al. (2010) Ciliary neurotrophic factor cell-based delivery prevents synaptic impairment and improves memory in mouse models of Alzheimer's disease. *J Neurosci* 30(22):7516-7527.
7. Callizot N, Combes M, Steinschneider R, & Poindron P (2013) Operational dissection of beta-amyloid cytopathic effects on cultured neurons. *J Neurosci Res* 91(5):706-716.